Biomaterials 129 (2017) 188–198

Contents lists available at ScienceDirect

Biomaterials

journal homepage: www.elsevier.com/locate/biomaterials

Development of a UV crosslinked biodegradable hydrogel containing adipose derived stem cells to promote vascularization for skin wounds and tissue engineering

Gozde Eke [a, d, g, 1], Naside Mangir [e, f, 1], Nesrin Hasirci [a, b, d], Sheila MacNeil [e], Vasif Hasirci [a, c, d, *]

[a] Middle East Technical University (METU), Department of Biotechnology, 06800 Ankara, Turkey
[b] METU, Department of Chemistry, 06800 Ankara, Turkey
[c] METU, Department of Biological Sciences, 06800 Ankara, Turkey
[d] BIOMATEN, METU Center of Excellence in Biomaterials and Tissue Engineering, 06800 Ankara, Turkey
[e] Department of Materials Science & Engineering, The Kroto Research Institute, University of Sheffield, Broad Lane, S3 7HQ Sheffield, United Kingdom
[f] Royal Hallamshire Hospital, Urology Clinic, Sheffield, United Kingdom
[g] Ahi Evran University, Department of Chemistry, Faculty of Arts and Sciences, 40100 Kirsehir, Turkey

ARTICLE INFO

Article history:
Received 13 December 2016
Received in revised form
13 March 2017
Accepted 13 March 2017
Available online 18 March 2017

Keywords:
Dermal substitute
Bicomponent hydrogel
Adipose derived stem cells
Photocrosslinking
Angiogenesis

ABSTRACT

The aim of this study was to design a dermal substitute containing adipose derived stem cells (ADSC) that can be used to improve the regeneration of skin on difficult wound beds by stimulating rapid neovascularization. This was achieved by first synthesizing methacrylated gelatin (GelMA) and methacrylated hyaluronic acid (HAMA) precursors which could be stored at −80 °C after lyophilisation. Polymer precursors were then dissolved in media (in 15:1 ratio), ADSCs added together with the photoinitiator and crosslinked with 40 s of UV. Hydrogels degraded by 50% over 3 weeks in an *in vitro* environment. ADSC loaded hydrogels could be easily handled with forceps (compressive modulus was 6 kPa). Transparency of the gel would allow a full field-of-view of a wound site. The hydrogels provided a suitable microenvironment for ADSC proliferation as shown by the filopodia observed in confocal micrographs. *In vivo* studies demonstrated that stem cell loaded hydrogels increased vascularization by up to 3 fold compared to their cell free counterparts. In conclusion, GelMA/HAMA hydrogels loaded with ADSC showed the desired proliferative and angiogenic properties essential to promote angiogenesis for wound healing and improving survival of tissue engineered skin.

1. Introduction

Skin is the largest organ in the human body accounting for nearly 10% of the body weight. Loss of normal barrier and thermoregulatory functions of skin can have devastating consequences in patients with burns, trauma and chronic wounds secondary to diabetes or venous insufficiency. Patients who lost larger than 4 cm in diameter of their full thickness skin will require an autologous split thickness skin graft from elsewhere on their body. In cases where the loss is extensive tissue engineered skin is then called on. The currently available tissue engineered and cell-based treatment strategies have been reviewed previously [1].

Tissue engineered skin has been under development since the early 1980s. It is now possible to make skin grafts constituted of both the epidermal and the dermal layers, however, one area that remains a challenge is their "take" and survival on wound beds after implantation. In a pilot clinical study from our group, in 4 of the 6 patients treated with tissue engineered skin based on de-epidermised, decellularised, cadaveric donor dermis reconstructed with autologous keratinocytes and fibroblasts, these grafts were eventually lost due to delayed vascularization [2]. In contrast, when a similar construct, tissue engineered buccal mucosa, was grafted onto a well vascularized wound bed to treat scarring of the urethra (urethral stricture disease) we could demonstrate excellent grafting [3]. Taken together these confirm the point that survival of tissue engineered skin grafts depend heavily on the rapid ingrowth of blood vessels from the underlying wound bed.

* Corresponding author. Middle East Technical University, Department of Biological Sciences, 06800 Ankara, Turkey.
E-mail address: vhasirci@metu.edu.tr (V. Hasirci).
[1] Joint first authors.

http://dx.doi.org/10.1016/j.biomaterials.2017.03.021
0142-9612/

Converting a poorly vascularized wound bed to a well vascularised wound bed prior to grafting of a tissue engineered skin has been recognized and adopted for a long while. In practice, those groups which have made most clinical progress in this area [4] have advocated prior treatment of the wound bed, as part of a two stage operation, with a material such as Integra® [5]. This resulted in a very impressive take of cultured skin substitutes in patients with full thickness burns. Another strategy to promote vascularisation of tissue engineered constructs can be incorporating mesenchymal stem cells (MSCs) into it [6]. A number of studies, including some work from our laboratory, have looked at ways of delivering MSCs to wound bed. We described a 2D carrier for delivering MSCs confirming that their activity after they are transferred to a wound bed remains unchanged [7] and these were then assessed for their ability to promote wound healing in a diabetic mouse model where the results were consistent with MSCs acting in a pro-angiogenic capacity [8].

It was also shown by our group in a bilayer tissue engineered oral mucosal substitute that mesenchymal cell type used in a dermal layer has an important effect on epithelial cells in controlling epithelial development. Mesenchymal cells of different sources (oral, dermal, and corneal fibroblasts) showed that the cell source had a significant influence on the thickness and ultrastructure of the epithelial layer [9].

In the current study we take on the challenge of developing a dermal substitute which contains MSCs that can be used in a two stage procedure to improve the take and survival of tissue engineered skin. The requirements for this dermal substitute are that it should be biocompatible, biodegradable, have good handling characteristics, be easy to assemble with MSCs in the laboratory and critically support the growth and survival of MSC capable of stimulating angiogenesis. It must also be simple to use in the clinic. The latter is important as methodologies of delivering MSCs that are not surgeon friendly are unlikely to be adopted.

Hydrogels meet most of these requirements as dermal substitutes and are commonly used as wound dressings due to their good viscoelasticity and water content.

Hyaluronic acid is a polysaccharide with high water retention capacity and elasticity, and abundant in shape forming tissues such as nose and ear, and in joints where they also function as lubricants. It is not adhesive for cells and therefore used in lower quantities in hydrogels than collagen or gelatin in tissue engineering applications. Hyaluronic acid is effective in wound healing and is a vital element of viscoelastic tissues.

Gelatin on the other hand, is a derivative of collagen and is frequently included in hydrogels because of its excellent gelling properties, biocompatibility and biodegradability. A limitation of gelatin based hydrogels, however, is their poor mechanical properties, particularly in terms of thermostability. These limitations can be overcome by chemical or physical crosslinking of gelatin. Also, gelatin based hydrogels can be enriched by adding other extracellular matrix (ECM) components such as hyaluronic acid. Previously, we showed that porous gelatin scaffolds carrying epidermal growth factor (EGF) lead to a fast and proper healing of full skin defects created on rabbits [10] and on diabetic rats [11]. We observed that the wound dressings prepared from Heparin-Chitosan-Alginate demonstrate very effective antibacterial property against *S. Epidermidis* [12]. In another study, we have shown that tissue engineering using biomolecules like collagen blended with synthetic polypeptides called ELR (elastin like recombinamer) lead to highly vascularized oral mucosa equivalents [13].

Bicomponent polymer network (BCN) hydrogels are unique structures that allow the combination of two independent networks to be integrated with each other resulting in better mechanical properties while preserving the desired properties of the original polymers.

In this study we hypothesized that gelatin and hyaluronic acid could be effectively crosslinked into a BCN hydrogel structure suitable for incorporating MSCs within them for delivery to wound beds to stimulate new blood vessel formation and for later use as the dermal layer of a bilayer skin substitute.

2. Materials and methods

2.1. Preparation of the gel

2.1.1. Synthesis of methacrylated gelatin (GelMA)

Methacrylated gelatin was synthesized according to the Nichol et al. (2010) [14]. Briefly, a solution of porcine skin gelatin type A (Sigma-Aldrich, UK) (10%, w/v) in phosphate buffer (10 mM, pH 7.4) was prepared. Methacrylic anhydride (Sigma-Aldrich, UK) (20%) was added dropwise into the gelatin solution at 50 °C and stirred for 1 h. Then, the mixture was diluted 5 fold with warm phosphate buffer (40 °C), filtered and dialysed against distilled water for 1 week and lyophilised (Labconco Freezone 6, USA) (Fig. 1A).

2.1.2. Synthesis of methacrylated hyaluronic acid (HAMA)

Methacrylated hyaluronic acid was prepared as described by Messager et al. (2013) [15]. Briefly, a solution of hyaluronic acid in distilled water (0.5 w/v, %) was prepared and DMF (dimethylformamide) was added to achieve a ratio of 3:2 H_2O:DMF. Methacrylic anhydride (1%) was added dropwise while stirring. pH was adjusted to ca. 8–9 with NaOH (0.5 M), incubated overnight at +4 °C with continuous stirring, dialysed against distilled water for 3 days and lyophilised (Fig. 1B).

2.1.3. Preparation of GelMA/HAMA bicomponent network (BCN) hydrogels

A solution of GelMA and HAMA was prepared in cell culture media in which the final concentrations of the polymers were 15 and 1% (w/v), respectively, yielding a 15:1 (w:w) ratio of the two polymers. Photoinitiator (Irgacure 2959, 0.3%, w/v) was added and placed in a PDMS mold (i.d. 1 cm). The solution was exposed to 365 nm UV (Omnicure s1000) for 40 s. After release from the molds, the hydrogels were washed with PBS (Fig. 1C).

2.2. Characterization of the hydrogels

2.2.1. NMR spectra of GelMA and HAMA hydrogels

High resolution proton nuclear magnetic resonance (^{1}H NMR) spectra of GelMA and HAMA were obtained at room temperature on a Bruker DPX 400 spectrometer operating at ^{1}H resonance frequency of 400 MHz, 16 scans and used to characterise GelMA and HAMA by the determination of their methacrylation degree.

The methacrylated biopolymer samples were dissolved in D_2O (30 mg/mL). The methacrylation degree is defined as follows [16]:

$$\text{Methacrylation degree } (\%) = \frac{\text{Number of methacrylate groups}}{\text{Number of amine groups on unreacted polymers}} \times 100 \quad (1)$$

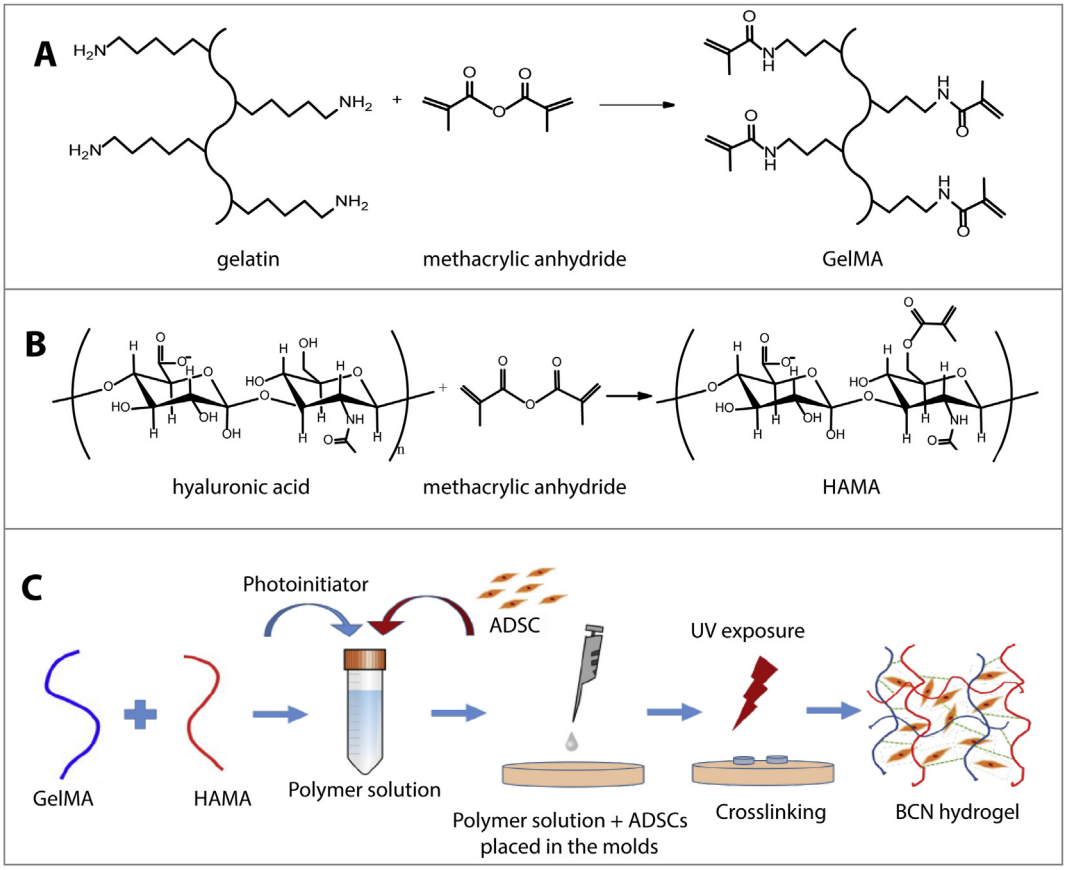

Fig. 1. Assembly of an ADSC containing hydrogel from GelMA and HAMA polymer chains. Prior to gel assembly, gelatin and hyaluronic acid are methacrylated separately and lyophilised for storage. A) The binding of methacrylate groups to the primary NH_2 groups of gelatin, B) The binding of methacrylate groups to the hydroxyl groups of hyaluronic acid. C) To create a bicomponent hydrogel, a solution of methacrylated gelatin and methacrylated hyaluronic acid was formed by rehydrating lyophilised powders of both in media alone (control hydrogel) or media containing cells (cell-containing hydrogel) then crosslinked by the addition of a photoinitiator and UV irradiation for 40 s.

2.2.2. Morphology and porosity analysis by SEM

Hydrogels were frozen in liquid nitrogen, lyophilised and sputter coated with Au-Pd (2 nm) and examined with QUANTA 400F field emission SEM (Netherland). Porosity and pore sizes were calculated with Image J software (NIH). Each group had 3 hydrogel samples. 5 images from each sample were randomly selected and 5 measurements from each image were taken.

2.2.3. Mechanical testing

Compressive mechanical tests were performed on a universal test machine (Shimadzu AGS-X, Japan) at room temperature. Hydrogels were kept in PBS for swelling prior to the testing. The crosshead speed was 1 mm/min. The applied force (F), cross-sectional area (A), initial sample length (l) and the displacement (Δl) measured during the experiments were used to calculate the stress ($\sigma = F/A$), the strain ($\varepsilon = \Delta l/l$), and compressive modulus (σ/ε).

2.2.4. Transparency

Transmittance (T) of the BCN hydrogels was measured in the range 250–700 nm with 5 nm intervals (n = 5) using a UV–Vis spectrophotometer (Thermo Scientific, USA).

2.2.5. In situ degradation

The test was performed according to ASTM F 1635-04a on each hydrogel formulation. Pre-weighed hydrogels were placed in sterile PBS and weighed daily after lyophilisation.

2.2.6. Swelling

The degree of swelling (DS) of the GelMA/HAMA hydrogels were calculated from the weights of the samples in dry and wet states after 48 h in PBS. DS was calculated according to the following equation:

$$DS(\%) = \frac{w_s - w_d}{w_s} \times 100 \quad (2)$$

where w_s is swollen weight and w_d is dry weight of the hydrogels.

2.3. In vitro studies

Adipose derived stem cells (ADSCs) were a kind gift from Dr. Sabiniano Roman and were isolated from human subcutaneous fat tissue from abdominoplasties (covered under a Human Tissue Authority research tissue bank license: 08/H1308/39, England) and used up to passage 5. Cells were cultured as previously described [17].

ADSCs ($0.5 \times 10^6 - 2 \times 10^6$ cells) were resuspended in GelMA/HAMA polymer solution (200 μL) containing 0.5% (w/v) photoinitiator and the BCN hydrogels (GelMA/HAMA) were produced as described in Section 2.1.3.

In some tests VEGF (100 ng/hydrogel) was added into the hydrogel composition as a positive control of ADSC presence.

2.3.1. Viability of ADSCs in the hydrogels assessed by Live-Dead assay

Hydrogels loaded with ADSCs were cultured for 3 weeks, washed with PBS and double stained with calcein AM (4 μM in PBS) and ethidium homodimer-1 (10 μM in PBS) for 20 min. Excess stain was removed, gels were washed with PBS, and examined by confocal microscopy (CLSM, Zeiss LSM 9100, Germany).

2.3.2. Cell proliferation by total DNA quantification assay

Total DNA of the ADSCs was isolated at each time point using a Genomic DNA Purification Kit (Promega, USA) according to the manufacturer's protocol. Total DNA isolated was quantified (n = 5) with PicoGreen dsDNA Assay (Invitrogen, USA). The samples and DNA standards (10 μL) were incubated with PicoGreen reagents and fluorescence was measured at 560/590 nm (excitation/emission), and DNA content was determined.

2.3.3. Assessment of ADSC behaviour in the BCN hydrogels

Behaviour of ADSCs in the hydrogels at different time points were studied with CLSM. Cytoskeleton and nuclei of the cells were stained with Alexa488 (λ_{ex}: 495 nm, λ_{em}: 519 nm) and Draq5 (λ_{ex}: 646 nm, λ_{em}: 697 nm), respectively and observed with 20× and 40× objectives.

2.4. Evaluation of angiogenic potential of the BCN hydrogel

The angiogenic potential of the BCN hydrogels was studied with 2 different assays, chick aortic arch assay and chick chorioallontoic membrane (CAM) assay.

2.4.1. Incubation of eggs

Pathogen-free fertilized white leghorn chicken eggs (*Gallus gallus domesticus*) were obtained from Henry Stewart Co. Ltd (UK). Care was consistent with the guidelines of the Home Office, UK. Chick embryos were cultured as described previously [18] except this time an ex ovo (shell less) culture method was used [19]. The egg shells were cracked and embryos were transferred into a square petri dish on embryonic development day (EDD) 3. The *ex ovo* cultures were maintained in a humidified incubator at 38 °C between EDDs 3 to 14. The survival of the embryos was checked daily and recorded.

2.4.2. The chick aortic arch assay

Chicken embryos were sacrificed on EDD 14, aortic arches removed aortic branches were cut into 1 mm rings under a stereomicroscope. Aortic rings were embedded in 50 μL of Matrigel® (Basement Membrane Matrix, Corning®) in a 24 well plate. After 30 min of incubation, DMEM (2 mL, supplemented with 2.5% FCS, 50 units/mL penicillin and 50 μg/mL streptomycin, GIBCO, Carlsbad, CA) was added into each well and incubated in an incubator at 37 °C and 5% CO_2.

With the aid of a transparent tissue culture insert (Greiner Bio-One GmbH) the aortic rings were co-cultured with unloaded or ADSC loaded BCN hydrogels (2.5×10^5; 5×10^5 and 10×10^5 ADSCs were loaded in the hydrogels). The endothelial sprouts were observed under an inverted microscope on Day 5 and the longest sprout length for each sample was calculated, as described previously [20]. Endothelial cells were characterized by immunofluorescence staining with Griffonia Simplicifolia Lectin I, isolectin B4 (Vector Laboratories, Burlingame, USA).

2.4.3. The ex ovo CAM assay

Unloaded, VEGF loaded and ADSC loaded BCN hydrogels with an internal diameter of 8 mm were prepared. At EDD 8, two gels from the same group were placed on the CAM surface at opposite sites. At EDD 14, pictures of hydrogel and surrounding CAM area were taken with a digital microscope. After imaging, embryos were sacrificed by cutting their vitelline arteries and gels were resected from the CAM surface with 1 cm margin.

2.4.4. Morphometric quantification of angiogenesis

Quantification of angiogenesis was performed on 6 digital images from each group using an online Image J plug-in, NeuronJ (Meijering et al., Cytometry Part A 2004; 58A:167–176; http://www. imagescience.org/meijering/software/neuronj/). The total number of vessels and total vessel length of all traced vessels were calculated together with a 'vasculogenic index' which is defined as all discernible blood vessels traversing a 1 mm annulus about the 2 mm imaginary circle drawn around the hydrogel [21].

2.5. Histology

The gels and surrounding CAM were fixed with formaldehyde (10%), embedded in paraffin and 6 μm sections were cut. Conventional haematoxylin and eosin (H&E) staining was performed. Slides were examined under light microscopy to see blood vessels and the inflammatory response in the CAM adjacent to hydrogels. Blood vessels were also stained with a conjugated alpha smooth muscle actin antibody (α-SMA, Sigma-Aldrich, UK) together with a 4′,6-diamidino-2-phenylindole dihydrochloride (DAPI, Gibco Invitrogen, UK) nuclei staining. Slides were observed under an epifluorescence microscope (Olympus, Japan) and the area of α-SMA stained blood vessels were measured (n = 6).

2.6. Statistical analysis

Statistical analysis was performed with Graphpad Prism6 programme. Differences between group means were analysed with Student's T test when the data was normally distributed. Mann Whitney *U* test was used for data that was not normally distributed. Comparisons of more than 2 groups were performed with One-way ANOVA with Tukey's post-hoc test, to determine significant differences. All values are represented as the mean ± standard deviation. Differences were taken to be significant for $p < 0.05$.

3. Results

3.1. Characterization of hydrogels

3.1.1. Methacrylation of gelatin and hyaluronic acid

The degree of methacrylation of gelatin was calculated from the peaks of spectrum obtained from the proton NMR at 7.4 ppm for the aromatic amino acid residues of gelatin, and the peaks at 5.5 ppm and 5.7 ppm for the double bonds of the methacrylate groups [14,16] (Fig. 2A).

The methacrylation reaction of hyaluronic acid showing the methacrylate peaks at 6.1, 5.6, and 1.85 ppm (Fig. 2B) presents a proton NMR spectrum characteristic for this reaction [15]. The degree of methacrylation was calculated from the relative integrated intensities of the methacrylate protons and methyl protons in hyaluronic acid (peak at 1.9 ppm). NMR results demonstrated that gelatin was 63% methacrylated and hyaluronic acid 25% methacrylated (Fig. 2A and B). Thus, the efficiency of gelatin methacrylation was about 2.5-fold higher than that of hyaluronic acid.

3.1.2. Morphology of GelMA/HAMA BCN hydrogels

BCN hydrogel was obtained after the methacrylated gelatin and hyaluronic acid solutions were mixed and crosslinked with UV (Fig. 3). The GelMA and HAMA solutions were free-flowing before

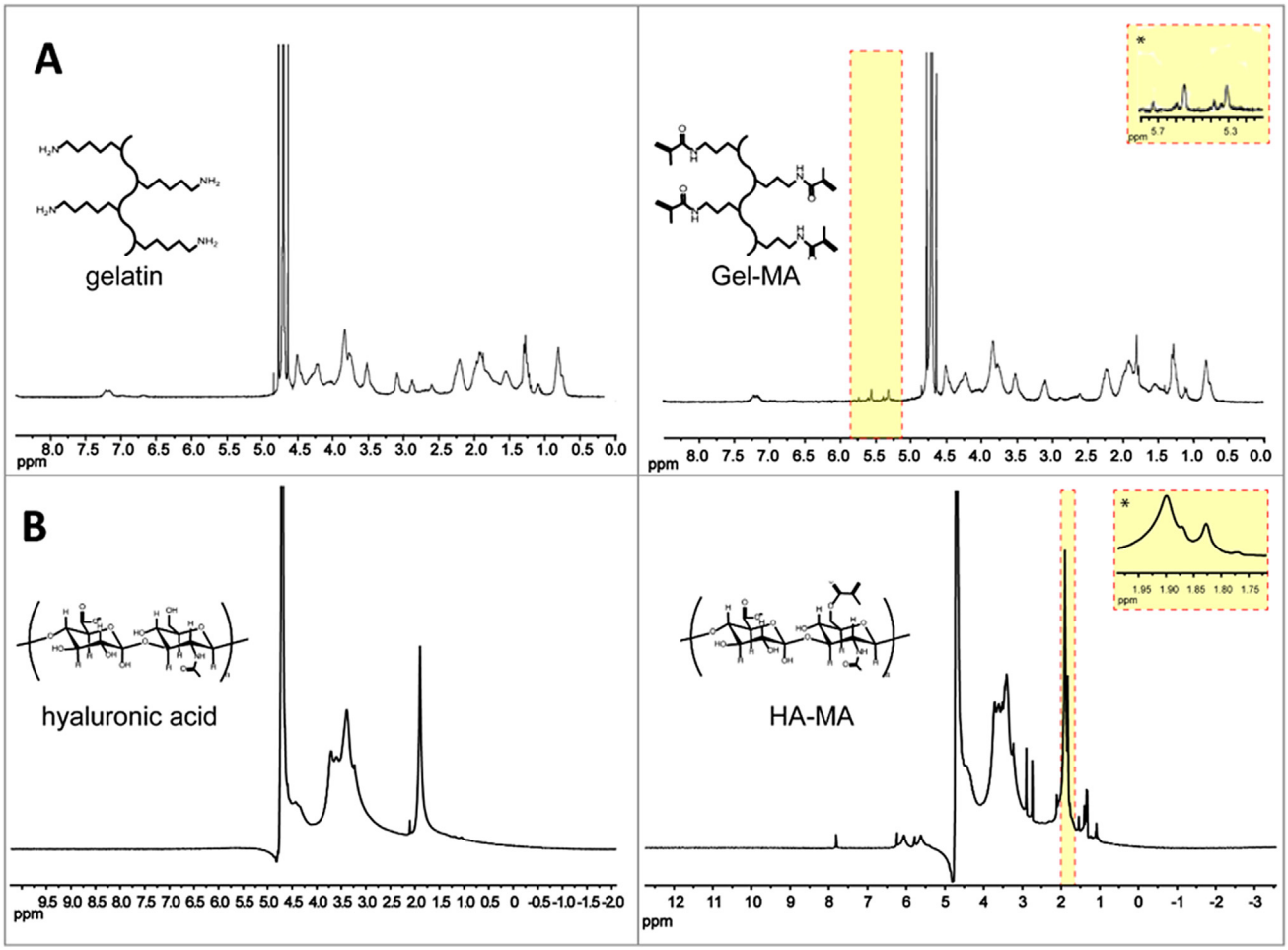

Fig. 2. ^{1}H NMR spectra of gelatin, hyaluronic acid and their methacrylamide forms prepared in D_2O at room temperature. A) ^{1}H NMR spectra of gelatin (left) and gelatin methacrylamide (Gel-MA) (right). The expanded region in Gel-MA between 5 and 6 ppm (shown with an asterix) is presented as insets which show the methacrylation of gelatin. B) ^{1}H NMR spectra of hyaluronic acid (left) and hyaluronic acid methacrylamide (right). The expanded region between 1.5 and 2 ppm (shown with an asterix) represents the increase in the peaks because of methacrylation as shown at the inset.

UV exposure (Fig. 3A, left), and turned into a solid mass after crosslinking with UV (Fig. 3A, right). The 3D bulk structure of the GelMA/HAMA BCN hydrogel was shown with SEM to be highly porous (Fig. 3B). The average pore size was 120 ± 76 μm with 79% porosity (n = 75). Such pore size and the porosity are very suitable for tissue engineering applications.

3.1.3. Handling of the hydrogel and its mechanical properties

A round 1 cm-diameter piece of the BCN hydrogel could be easily manipulated using surgical forceps without breaking and deforming showing it was robust enough for handling (Fig. 3C).

In compression testing, the BCN hydrogels were stable until compression with a load of 12.86 ± 1.23 kPa and had a modulus of 6.17 ± 2.05 kPa.

3.1.4. Swelling and in situ degradation

Hydrogels are a crosslinked network of hydrophilic polymers that can swell in water to capture many times their original mass and can undergo hydrolytic degradation in aqueous environments. The hydrogels reached equilibrium swelling after about 48 h. The degree of swelling (DS) of the hydrogels was calculated as 227% ± 11 (n = 5).

The weight loss over time was used as a measure of degradation. Measurable differences in weights were observed, initially at a slow rate and after the first week at a higher rate. GelMA/HAMA hydrogels lost 50% of their weight during the 21 days in PBS at 37 °C in an incubator and rotated at a rate of 70 rpm (Fig. 3D).

3.1.5. Transparency

The transmittance analysis of unloaded and ADSC loaded BCN hydrogels show that the unloaded hydrogels have 85% light transmittance in the visible spectrum allowing a full field-of-view of the wound site at all times (Fig. 3E and F). Loading the stem cells into the BCN hydrogel did not significantly affect the transmittance up to a loading of 1 million ADSCs. The transmittance decreased to 56% in the visible range when 2 million cells were loaded. All samples transmitted very low UV light at wavelengths of 320–400 nm (UVA) and 290–320 nm (UVB).

3.2. In vitro studies

3.2.1. Viability of ADSCs in the hydrogels by Live-Dead assay

On Live-Dead Cell staining, live cell (green) coverage was 99, 97, 94 and 96% on days 3, 7, 14 and 21, respectively (Fig. 4A) showing that more than 90% of the cells were alive, able to elongate and move freely in the hydrogels for 3 weeks.

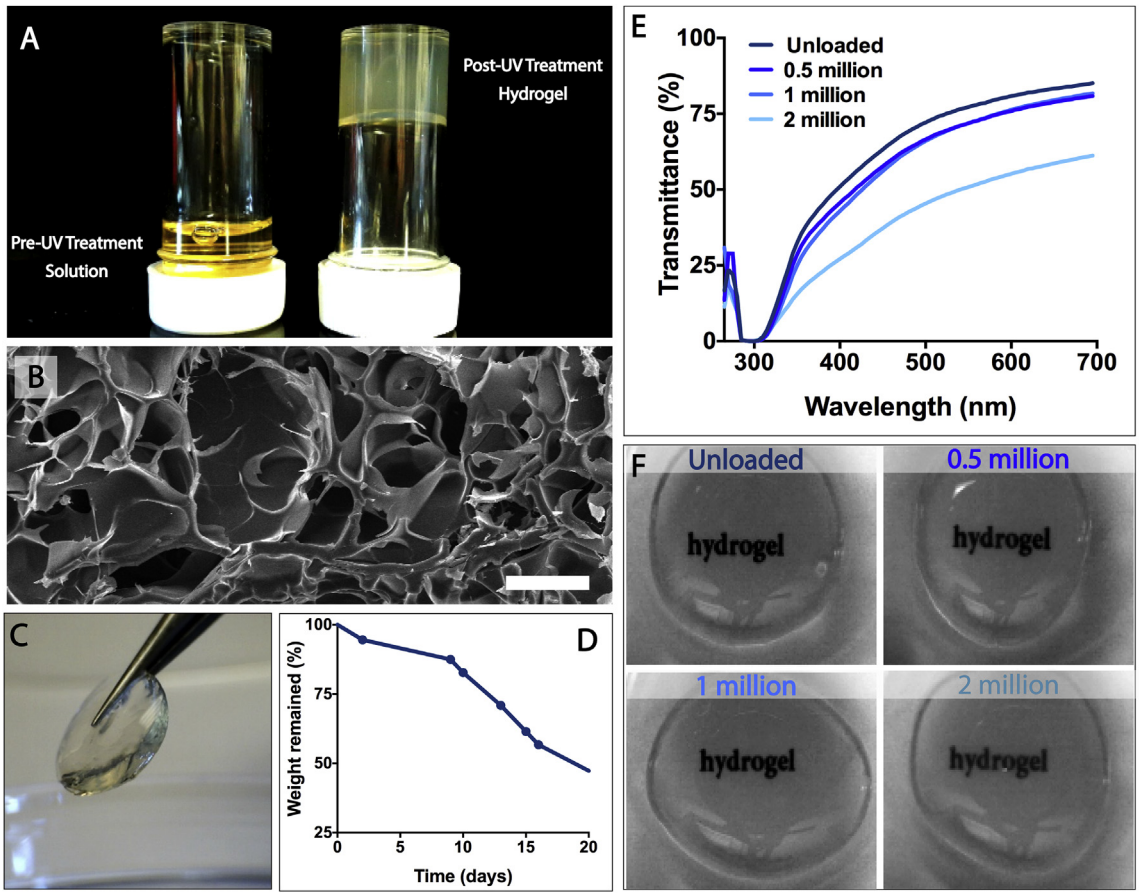

Fig. 3. Characterization of BCN hydrogels. A) BCN gel solution before (left) and after (right) 50 s of UV treatment, B) SEM of the cross-section of the BCN hydrogel (scale bar: 100 μm). C) Photograph showing easy handling of the BCN hydrogel with surgical forceps, D) *In situ* weight loss from the hydrogel over 21 days, E) Transparency of the hydrogel. Up to 2 million cells in the BCN gel did not significantly affect the transparency of the gel. The BCN hydrogel does not transmit light in the ultraviolet region making it inherently sun protective. F) A decrease in the transparency of the hydrogels with an increasing number of cells. Opacity increases with the loading of 2 million cells.

3.2.2. Cell proliferation and DNA quantification in hydrogels

The amount of DNA after 3 weeks of *in vitro* culture was determined by quantification of DNA with PicoGreen staining (Fig. 4B). It was observed that ADSCs in the hydrogels proliferated at a rate similar to that in 2D culture on TCPS and gradually increased throughout the 21 day incubation. There was a gradual increase in the amount of DNA over the 21 days of culture indicating cell proliferation in the hydrogels.

3.2.3. Determination of ADSC morphology in the hydrogels

After 3 days in culture, ADSCs encapsulated in the GelMA/HAMA BCN hydrogels started to spread and form protrusions into the hydrogels (Fig. 5A). On Day 14, they appeared more elongated, and by Day 21 formed interconnected networks with the neighbouring cells. Pore size and porosity of the hydrogels were measured from their SEM using NIH imageJ program. Porosity increased from 130 ± 72 on Day 3–210 ± 98 μm on Day 21 (Fig. 5B) indicating the degradation of the hydrogel.

3.3. The angiogenic potential of BCN hydrogel

The sprouting tubular structures observed in the chick aortic ring assay were identified as endothelial cells as they stained positively with the endothelial cell marker Isolectin B4 (Fig. 6A). A significant increase in the length of the endothelial cell sprouts when co-cultured with ADSC loaded BCN hydrogels was observed unlike the unloaded hydrogels (Fig. 6B). Also an effective concentration for ADSCs to increase endothelial cell sprouts was found to be between 5×10^5 - 1×10^6 (Fig. 6C).

The CAM assay clearly demonstrated newly growing blood vessels towards ADSC loaded and VEGF loaded BCN hydrogels where unloaded hydrogels served as controls (Fig. 7A). The total number and length of blood vessels growing on the CAM tissue adjacent to the VEGF loaded and ADSC loaded hydrogel was significantly higher compared to unloaded ones. Also, the vasculogenic index (number of vessels growing towards the gel in a spoke-wheel pattern) was highest for VEGF loaded hydrogels and ADSC loaded hydrogels was the second highest with unloaded hydrogels being the lowest (Fig. 7B).

3.4. Histological evaluation of angiogenesis and initial in vivo tissue response to BCN hydrogels

Histological and immunohistological evaluation of normal CAM structure is demonstrated in Fig. 8A. Histologic examination of CAM-hydrogel complex have confirmed a significantly increased area of α-SMA positive blood vessels in CAM tissue under and adjacent to the VEGF loaded hydrogel compared to the hydrogel alone whereas ADSC loaded hydrogel was associated with a moderate increase in the number of blood vessels (Fig. 8B and C). Also the H&E staining of the samples demonstrated almost no inflammation in the CAM underneath the hydrogel and VEGF loaded hydrogel whereas a mild inflammatory response together with infiltration of inflammatory cells in the

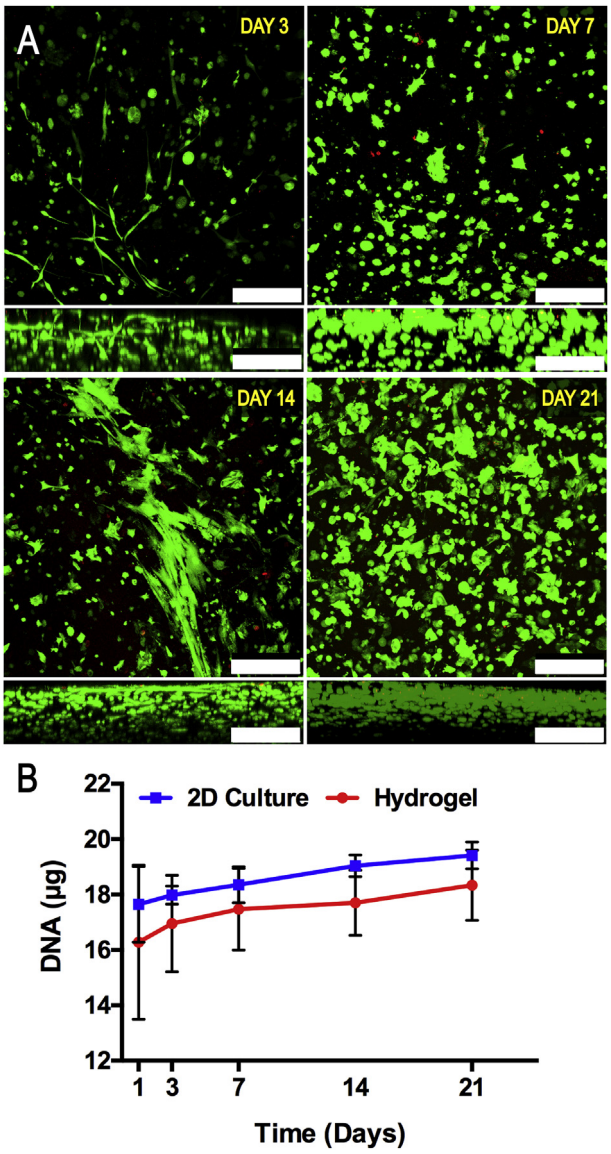

Fig. 4. Viability and proliferation of ADSC in the hydrogels. A) Live-Dead analysis of ADSCs using CLSM, on BCN hydrogels at different time points (3–21 days). Hydrogels stained with calcein AM for live and ethidium homodimer-1 for dead cells (Magnification ×10). Lower micrographs are the z-stacks of the micrographs showing the level of penetration of the ADSCs in the hydrogel (Scale bar: 250 µm). B) Quantification of DNA content by staining with PicoGreen. DNA of the ADSCs in the hydrogels was extracted at different time points and determined with fluorescence intensity measurements at 560/590 nm (excitation/emission). The number of cells in the hydrogels and on the TCPS (2D culture of the cells) were similar and statistically insignificant at each time point showing that the cell survival in the hydrogels was similar compared to control cells (Anova One-Way Tukey test, p: 0.014).

perivascular area was observed consistently in the ADSC loaded hydrogel group (Fig. 8C).

4. Discussion

In this study we synthesized and characterized a gelatin/hyaluronic acid based UV crosslinkable bicomponent (BCN) hydrogel that allows effective incorporation of stem cells within them that allows us to deliver cells to stimulate new blood vessel formation *in vivo*. This biodegradable hydrogel was designed to improve the take of tissue engineered skin when used in a two stage operation and also as the dermal layer for a bilayer skin substitute. Such an MSC containing hydrogel would also be valuable in stimulating blood vessel formation in poorly vascularized chronic wounds-a growing burden for patients and healthcare providers worldwide [22,23].

The main findings of the study are that one can readily combine ADSC with the GelMA/HAMA BCN hydrogels using only 40 s of UV crosslinking. Cells increase in number in this hydrogel over three weeks and stimulate new blood vessel formation assessed using an ex ovo CAM assay. This hydrogel is easy to handle and transparent.

A "bicomponent network" (BCN) is a network system comprising of two chemically different polymer sequences that are covalently bonded via a single chemical bond. BCNs can be differentiated from interpenetrating networks which comprise two or more independent networks that cannot be separated without breaking covalent bonds [24]. BCNs allow combining the properties of two different polymers while preserving their desired qualities. In our BCN hydrogel we combined the mechanical and cell attractive properties of gelatin with unique water retention and viscoelastic features of hyaluronic acid by crosslinking them via their methacrylate groups with the application of UV. Among other chemical and physical crosslinking methods, UV crosslinking has the advantage of being rapid and reliable.

In situ degradation studies showed that 50% of the hydrogel eroded within 21 days showing that the BCN hydrogel has a stable structure in the short term but will breakdown within a few weeks *in vitro*. Prior studies with the commercial dermal substitute product Integra have shown that it takes at least 3 weeks or more for new blood vessels to grow into this product from the underlying wound bed [3,25]. We hypothesise that this rate of hydrogel degradation will be appropriate for it acting as a dermal substitute and also a biological wound dressing for stimulating chronic wounds to heal. Further, the fact that the hydrogels are reasonably transparent even when loaded with cells will enable clinicians to view the wound bed under the hydrogel and see the extent of new blood vessel formation.

Hydrogels absorb and retain large amounts of water which then affects solute diffusion, surface properties and mechanical properties [26]. The degree of swelling of hydrogels is dependent on the concentration of the polymer solution, the methacrylation degree and the ratio of the components. Nichol et al. (2010) and Oudshoorn et al. (2007) showed that the swelling ratio increased with decreasing degree of methacrylation because of a decrease in the crosslinkage allowing the increase in swelling capability of the hydrogel [14] [27].

The GelMA/HAMA hydrogels serve as a dynamic environment for the ADSCs to proliferate and deposit their pericellular and extracellular matrix. Hyaluronic acid, a nonsulfated glycosaminoglycan, has shown its versatility by being used for wound healing [28] and the involvement of hyaluronic acid in the hydrogel is important because it mimics the composition of the *in vivo* cellular environment and also acts as a promoter of early inflammation, which is crucial in the whole skin wound healing process. Mesenchymal stem cells have the ability to differentiate into various lineages as a result of physical, chemical and mechanical signals from their microenvironment. A limitation of this study is that the effect of the hydrogel microenvironment on the stemness of the MSCs have not been studied, however, previous studies suggest that the key mechanical guide in stem cell differentiation in hydrogels is the bulk matrix stiffness [29]. Our hydrogel can be considered rather soft (6 kPa) and this stiffness would not be expected to stimulate stem cell differentiation [30].

A relevant study evaluated the effect of different concentrations of gelatin and hyaluronic acid on physical and biological properties of a biomimetic hybrid hydrogel and demonstrated that addition of gelatin methacrylate (GelMA) into HA methacrylate (HAMA)

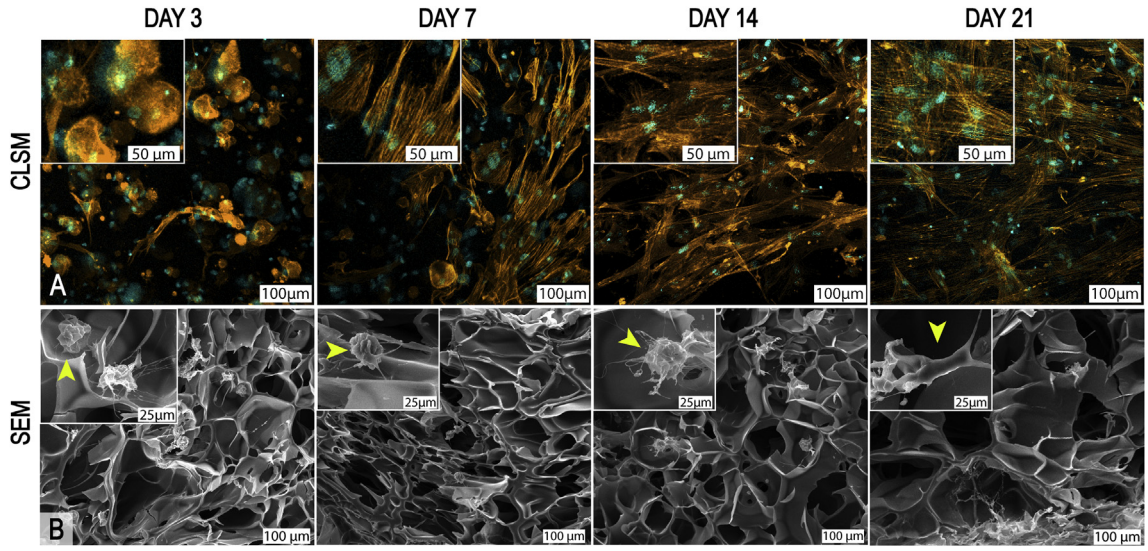

Fig. 5. Behaviour of ADSCs in the hydrogels at different time points as studied with CLSM and SEM. A) CLSM images of ADSC loaded hydrogels. Orange (Alexa488, cytoskeleton) and cyan (Draq5, nucleus). Filopodia were observed starting from Day 7. Magnification ×20. Cells are homogenously distributed inside the hydrogel. Inset micrographs show that the cells change from spherical to spindle like morphology. B) SEM micrographs show the cross-section of ADSC loaded hydrogels. Individual elongated cells could be seen starting from Day 7. Pore sizes and porosity of the hydrogel increased due to the *in vitro* degradation. Arrow heads in the insets show the change in cell morphology at different time points. (For interpretation of the references to colour in this figure legend, the reader is referred to the web version of this article.)

promoted cell spreading in the hybrid hydrogels [31]. Thus, it was necessary for us to initially explore various ratios of HA to gelatin as HA has been previously shown to resist cell adhesion for a few hours [32]. Once the cells were seeded, they initially tended to leak from the HA hydrogels. In order to obtain a cell adhesive HA carrying hydrogel with appropriate mechanical integrity, the ratio of HA to gelatin was adjusted to 1:15 and their concentrations in the final solution were 1% and 15%, respectively. With this HA to gelatin ratio the gels were cell friendly, easy to crosslink, transparent and easy to handle.

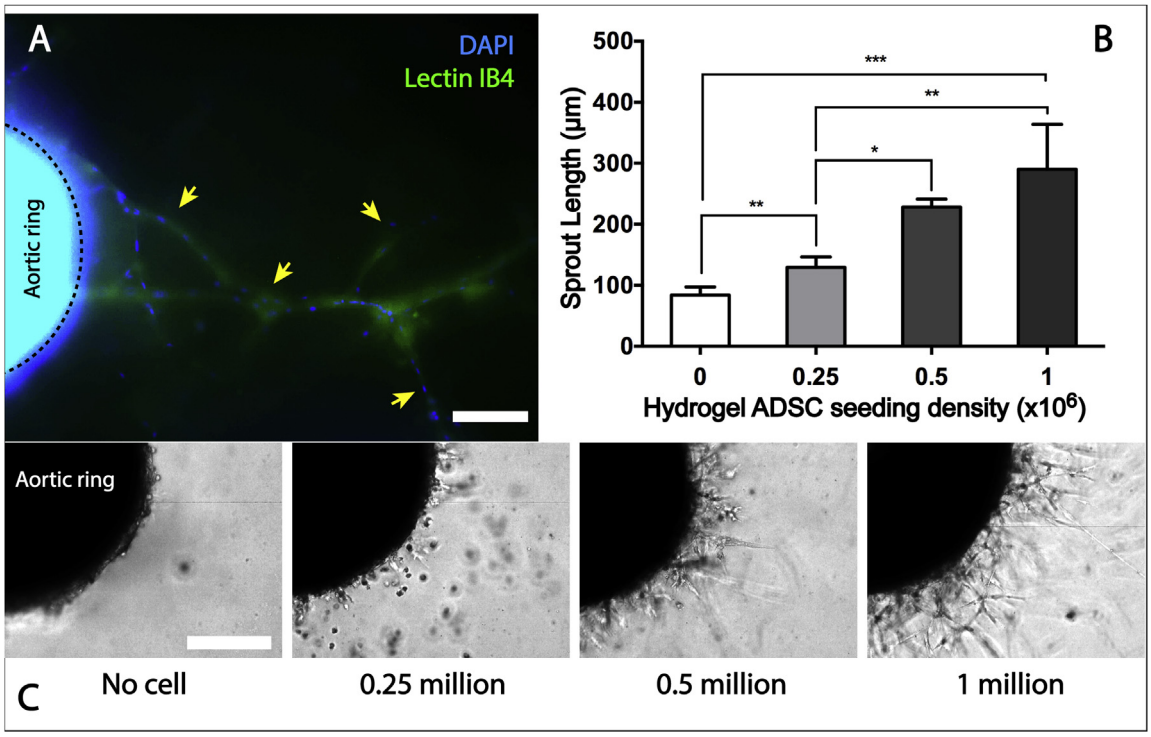

Fig. 6. ADSC loaded hydrogels were co-cultured with chick aortic arches to evaluate endothelial cell proliferation and sprouting on Day 5 of culture. A) Endothelial cell sprouts as observed with epifluorescence microscopy. Lectin IB4 positive endothelial cells are stained green, nuclear components stained blue (DAPI). Arrows show endothelial cell sprouts. B) The change in the length of endothelial sprouts with the seeding density of ADSCs. C) Micrographs for sprout length measurements used in the calculation of data for Fig. 6B (scale bars represent 250 µm). (For interpretation of the references to colour in this figure legend, the reader is referred to the web version of this article.)

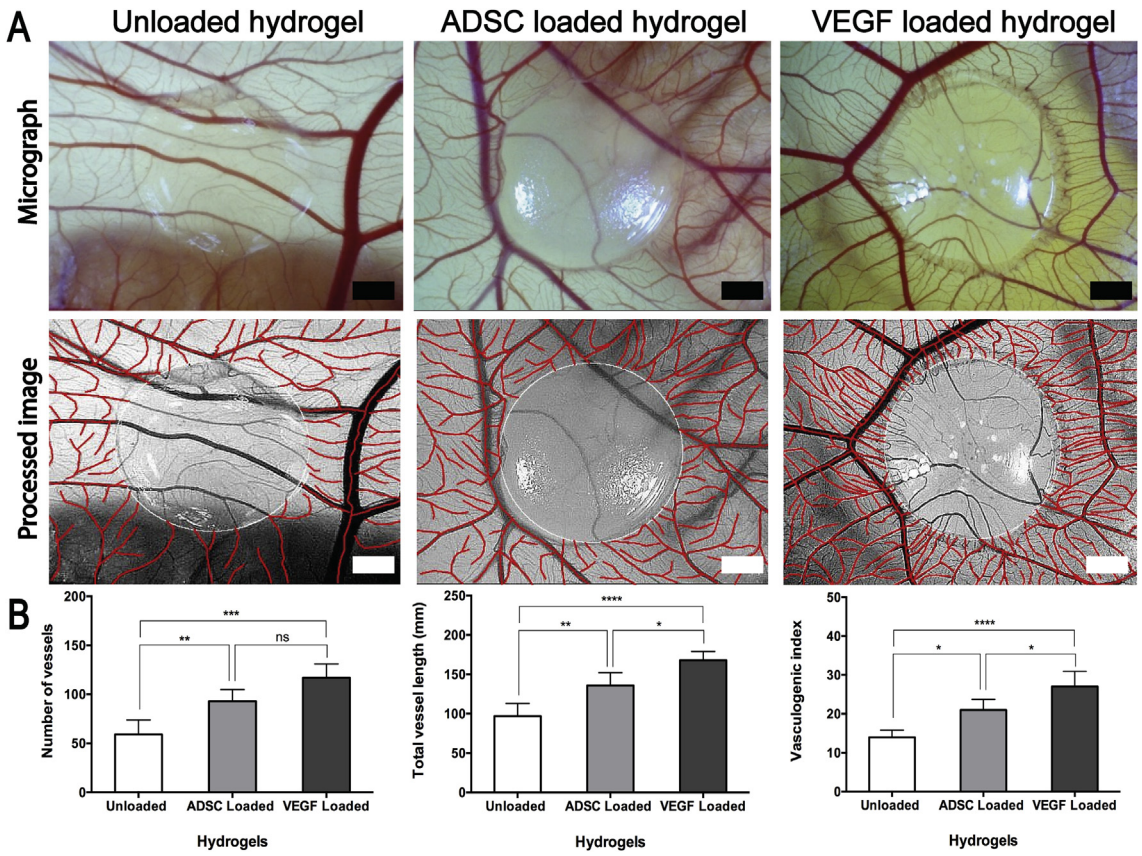

Fig. 7. Evaluation of the angiogenic properties of the BCN hydrogel in the chick chorioallantoic membrane (CAM) assay. A) Micrographs (upper row) and semi-automatic processed images (lower row) of the hydrogel, hydrogel containing ADSCs and hydrogel containing VEGF (positive control), taken on Day 14 of embryonic development. B) The change in total number of vessels, total vessel length and vascularization index of ADSC and VEGF loaded hydrogels calculated from processed images ($p < 0.005$, $n_{unloaded} = 5$, $n_{adsc\ loaded} = 4$, $n_{VEGF\ loaded} = 5$, One-way ANOVA, pairwise comparison Tukey's post-hoc test, *: $p < 0.05$, **: $p < 0.01$, ***: $p < 0.005$, ****: $p < 0.001$, ns: nonsignificant). Scale bars 2 mm.

In the literature GelMA hydrogels with concentration and degree of methacrylation similar to our study had a compressive modulus of about 10 kPa showing that our results are in line with previously published studies [14,33]. Also, the BCN hydrogels proved easy to handle and manipulate, which will be important in their handling in the laboratory and in the clinic in the future.

Another attractive feature of the GelMA/HAMA BCN hydrogel is its optical transparency. It is important to have a therapeutic device that can function as a wound dressing and transparent when wet and thus allows the follow up of the healing process without removing the dressing [26]. Another advantage of our hydrogel is its low transparency to UVA and UVB which makes it inherently protective against UV radiation. Whether the hydrogel will continue to remain transparent *in vivo* as it degrades will need to be investigated *in vivo*.

In designing the cell based hydrogel dressing to stimulate blood vessel formation it is important to consider how the cells will work, how long they need to be in place and the fate of the hydrogel in the long term. MSCs secrete a wide variety of pro-angiogenic factors such as vascular endothelial growth factor (VEGF), fibroblast growth factor 2 (FGF-2), and interleukin-6 (IL-6) that are shown to act at different steps of angiogenesis. Functionalization of tissue engineered constructs with stem cells to improve their vascularization has been investigated before [34,35]. Our study clearly demonstrates the BCN hydrogel *per se* had no effect on angiogenesis but when loaded with ADSC they increased the angiogenic response. ADSCs were not as effective as VEGF used as a positive control here. In other studies, degradation products of HA were demonstrated to increase angiogenesis, however, our results did not show an increased angiogenic response to control gels [36]. This may be due to the low concentration of HA used or possibly 7 days was not enough for the degradation products of HA to occur.

Currently the vasculogenic potential of tissue engineered materials are mainly evaluated by *in vivo* studies which do not allow direct visualization of the blood vessels and materials are expensive and the process is time consuming. The *ex ovo* CAM assay that we used in this study allows direct visualization of the newly forming vessels, is relatively rapid (within 2 weeks), and inexpensive. Also this method can potentially be used as a rapid, simple and low cost screening tool to test the initial tissue response to biomaterials, as a pre *in vivo* method [37]. Additionally, in this paper we have demonstrated an increasing number of endothelial cell sprouting from the chick aorta in response to an increasing number of ADSCs when they are co-cultured. Taken together our data suggests that it is the paracrine action of ADSCs, rather than the hydrogel, that promotes angiogenesis.

Finally, the link between neo-angiogenesis and inflammation has long been established. It is important to rule out inflammation as a trigger in angiogenesis, especially when xenogenic cell sources are studied. The chick embryo lacks a mature immune system, especially in the first 11 days of the embryonic development which appears as an advantage of using the CAM assay. Our histologic examination results proved that the BCN hydrogel alone did not cause any inflammation on the CAM tissue whereas ADSC loaded hydrogels caused a mild inflammatory reaction.

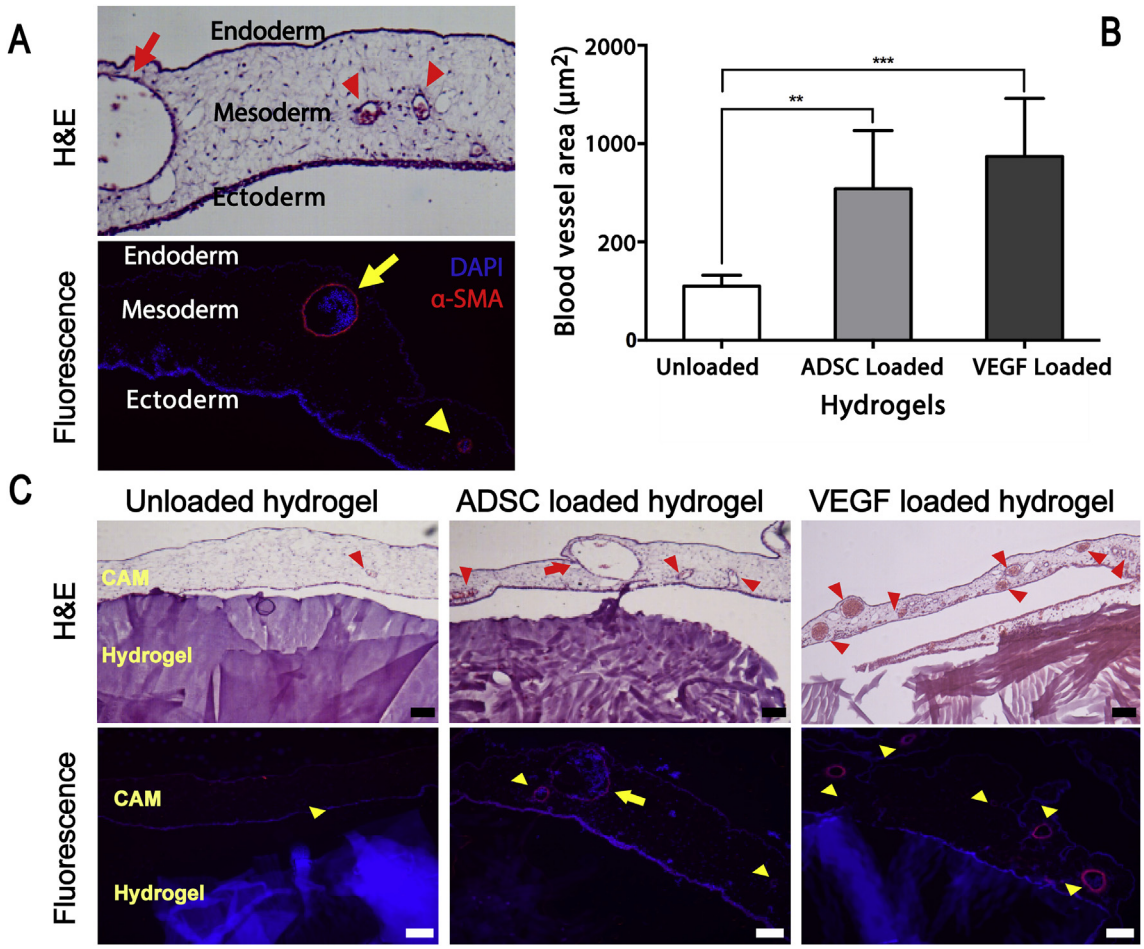

Fig. 8. Histological and immunohistological evaluation of angiogenic properties of BCN hydrogels on CAM at Day 14. A) Normal appearance of CAM structure on Haematoxylin &Eosin (H&E) staining and fluorescence staining of CAM vessels with alpha-smooth muscle actin (α-SMA) and 4′,6-diamidino-2-phenylindole dihydrochloride (DAPI). Arrows and arrow heads indicate large and small blood vessels, respectively. B) Bar chart showing quantification of fluorescent α-SMA positive blood vessel area (n = 5) where ADSC loaded hydrogels had significantly increased vessel area compared to unloaded hydrogel (One-way ANOVA, pairwise comparison Tukey's post-hoc test, **: $p < 0.01$, ***: $p < 0.005$). C) Representative images from each group demonstrating no inflammation and slight perivascular inflammatory cell infiltration on CAM tissue adjacent to unloaded and VEGF loaded BCN hydrogels and ADSC loaded hydrogels, respectively. Fluorescent stained images demonstrate more α-SMA stained blood vessels on the CAM underneath ADSC loaded and VEGF loaded hydrogels (Scale bars: 100 μm).

5. Conclusion

We conclude the GelMA/HAMA B hydrogel assessed in this study appears very promising when combined with ADSCs as an approach to provide a well vascularized dermis to improve the engraftment of tissue engineered skin. With respect to the possible future clinical applications, the proposed approach would be most clinically relevant in chronic non-healing wounds to stimulate wound healing.

This approach to achieve a vascularized dermis now merits further research in an *in vivo* animal model and prior to translation to the clinic issues of sterilisation of the hydrogel, the use of autologous or donor cells and the transport of cells from a GMP laboratory to the clinic will also need to be determined to translate this into a product to be tested in man.

Acknowledgments

The authors acknowledge Middle East Technical University Center of Excellence in Biomaterials and Tissue Engineering (BIOMATEN) for the use of the facilities and for the financial support, and METU Central Laboratory for SEM analysis. The authors also acknowledge TUBITAK 2211-C and 2214-A scholarships and Menekse Ermis Sen, MD, PhD, for statistical analysis. Naside Mangir was funded by the European Association of Urology Scholarship Programme (EUSP), The Rosetrees Trust and The Urology Foundation. We thank Dr. Sabiniano Roman for providing the cultured ADSC used in this study.

Appendix A. Supplementary data

Supplementary data related to this article can be found at http://dx.doi.org/10.1016/j.biomaterials.2017.03.021.

References

[1] S. MacNeil, Progress and opportunities for tissue-engineered skin, Nature 445 (2007) 874–880, http://dx.doi.org/10.1038/nature05664.
[2] P.S. Sahota, J.L. Burn, M. Heaton, E. Freedlander, S.K. Suvarna, N.J. Brown, S. Mac Neil, Development of a reconstructed human skin model for angiogenesis, Wound Repair Regen. 11 (2003) 275–284, http://dx.doi.org/10.1046/j.1524-475X.2003.11407.x.
[3] S. Bhargava, J.M. Patterson, R.D. Inman, S. MacNeil, C.R. Chapple, Tissue-engineered buccal mucosa urethroplasty-clinical outcomes, Eur. Urol. 53 (2008) 1263–1271, http://dx.doi.org/10.1016/j.eururo.2008.01.061.
[4] S.T. Boyce, R.J. Kagan, N.A. Meyer, K.P. Yakuboff, G.D. Warden, THE 1999 clinical research AWARD cultured skin substitutes combined with Integra

artificial skin* to replace native skin autograft and allograft for the closure of excised full-thickness burns, J. Burn Care Res. 20 (1999) 439–440, http://dx.doi.org/10.1097/00004630-199920060-00006.
[5] R. Stern, M. McPherson, M.T. Longaker, Histologic study of artificial skin used in the treatment of full-thickness thermal injury, J. Burn Care Rehabil. 11 (1990) 7–13, http://dx.doi.org/10.1097/00004630-199001000-00003.
[6] H. Naderi, M. Matin, A.R. Bahrami, Review paper: critical issues in tissue engineering: biomaterials, cell sources, angiogenesis, and drug delivery systems, J. Biomater. Appl. 26 (2011) 383–417, http://dx.doi.org/10.1177/0885328211408946.
[7] N.G. Walker, A.R. Mistry, L.E. Smith, P.C. Eves, G. Tsaknakis, S. Forster, S.M. Watt, S. Macneil, A chemically defined carrier for the delivery of human mesenchymal stem/stromal cells to skin wounds, Tissue Eng. Part C. Methods 18 (2012) 143–155, http://dx.doi.org/10.1089/ten.TEC.2011.0037.
[8] P. Jiang, W. Du, A. Mancuso, K. Wellen, X. Yang, Reciprocal regulation of p53 and malic enzymes modulates metabolism and senescence, Nature 33493 (2013) 689–693, http://dx.doi.org/10.1038/nature11776.
[9] B. Kinikoglu, R.M. Rovere, M. Haftek, V. Hasirci, D. Odile, Influence of the mesenchymal cell source on oral epithelial development, J. Tissue Eng. Regen. Med. 6 (2012) 245–252, http://dx.doi.org/10.1002/term.426.
[10] K. Ulubayram, A.N. Cakar, P. Korkusuz, C. Ertan, N. Hasirci, EGF containing gelatin-based wound dressings, Biomaterials 22 (2001) 1345–1356, http://dx.doi.org/10.1016/S0142-9612(00)00287-8.
[11] S. Dogan, S. Demirer, I. Kepenekci, B. Erkek, A. Kiziltay, N. Hasirci, S. Müftüoğlu, A. Nazikoğlu, N. Renda, U.D. Dincer, A. Elhan, E. Kuterdem, Epidermal growth factor-containing wound closure enhances wound healing in non-diabetic and diabetic rats, Int. Wound J. 6 (2009) 107–115, http://dx.doi.org/10.1111/j.1742-481X.2009.00584.x.
[12] A.E. Aksoy, U.A. Sezer, F. Kara, N. Hasirci, Heparin/Chitosan/alginate complex scaffolds as wound dressings: characterization and antibacterial study against S. Epidermidis, J. Biomater. Tissue Eng. 5 (2015) 104–113, http://dx.doi.org/10.1166/jbt.2015.1296.
[13] B. Kinikoglu, O. Damour, V. Hasirci, Tissue engineering of oral mucosa: a shared concept with skin, J. Artif. Organs 18 (2015) 8–19, http://dx.doi.org/10.1007/s10047-014-0798-5.
[14] J.W. Nichol, S.T. Koshy, H. Bae, C.M. Hwang, S. Yamanlar, A. Khademhosseini, Cell-laden microengineered gelatin methacrylate hydrogels, Biomaterials 31 (2010) 5536–5544, http://dx.doi.org/10.1016/j.biomaterials.2010.03.064.
[15] L. Messager, N. Portecop, E. Hachet, V. Lapeyre, I. Pignot-Paintrand, B. Catargi, R. Auzely-Velty, V. Ravaine, Photochemical crosslinking of hyaluronic acid confined in nanoemulsions: towards nanogels with a controlled structure, J. Mater. Chem. B Mater. Biol. Med. 1 (2013) 3369–3379, http://dx.doi.org/10.1039/c3tb20300j.
[16] H. Shin, B.D. Olsen, A. Khademhosseini, The mechanical properties and cytotoxicity of cell-laden double-network hydrogels based on photocrosslinkable gelatin and gellan gum biomacromolecules, Biomaterials 33 (2012) 3143–3152, http://dx.doi.org/10.1016/j.biomaterials.2011.12.050.
[17] S. Roman, A. Mangera, N. Osman, A.J. Bullock, C.R. Chapple, S. MacNeil, Developing a tissue engineered repair material for treatment of stress urinary incontinence and pelvic organ prolapse—which cell source? Neurourol. Urodyn. 33 (2014) 531–537, http://dx.doi.org/10.1002/nau.22443.
[18] G. Gigliobianco, C.K. Chong, S. MacNeil, Simple surface coating of electrospun poly-L-lactic acid scaffolds to induce angiogenesis, J. Biomater. Appl. 0 (2015) 1–11, http://dx.doi.org/10.1177/0885328215569891.
[19] R. Auerbach, L. Kubai, D. Knighton, J. Folkman, A simple procedure for the long-term cultivation of chicken embryos, Dev. Biol. 41 (1974) 391–394, http://dx.doi.org/10.1016/0012-1606(74)90316-9.
[20] A.N. Stratman, D.J. Kim, A. Sacharidou, K.R. Speichinger, G.E. Davis, The Textbook of Angiogenesis and Lymphangiogenesis, Methods Appl. (2012) 101–126, http://dx.doi.org/10.1007/978-94-007-4581-0.
[21] R.L. Barnhill, T.J. Ryan, Biochemical modulation of angiogenesis in the chorioallantoic membrane of the chick embryo, J. Invest Dermatol 81 (1983) 485–488.
[22] M. Chen, M. Przyborowski, F. Berthiaume, Stem cells for skin tissue engineering and wound healing, Crit. Rev. Biomed. Eng. 37 (2009) 399–421, http://dx.doi.org/10.1615/critrevbiomedeng.v37.i4-5.50.
[23] C. Tong, H. Hao, L. Xia, J. Liu, D. Ti, L. Dong, Q. Hou, H. Song, H. Liu, Y. Zhao, X. Fu, W. Han, Hypoxia pretreatment of bone marrow-derived mesenchymal stem cells seeded in a collagen-chitosan sponge scaffold promotes skin wound healing in diabetic rats with hindlimb ischemia, Wound Repair Regen. 24 (2015) 45–56, http://dx.doi.org/10.1111/wrr.12369.
[24] M.A. Sherman, J.P. Kennedy, Novel polyisobutylene/poly (dimethylsiloxane) bicomponent networks. I. Synthesis and characterization, J. Polym. Sci. Part A Polym. Chem. 36 (1998) 1891–1899, http://dx.doi.org/10.1002/(SICI)1099-0518(199808)36:11<1901::AID-POLA25>3.0.CO;2-H.
[25] E. Dantzer, F.M. Braye, Reconstructive surgery using an artificial dermis (Integra): results with 39 grafts, Br, J. Plast. Surg. 54 (2001) 659–664, http://dx.doi.org/10.1054/bjps.2001.3684.
[26] N. Hasirci, C. Kilic, A. Komez, G. Bahcecioglu, V. Hasirci, Hydrogels in regenerative medicine, in: M.R. Abidian, U.A. Gurkan, F. Edalat (Eds.), Handb. Polym. Appl. Med. Med. Devices, second ed., Worls Scientific, USA, 2016, pp. 1–52, http://dx.doi.org/10.1016/B978-0-323-22805-3.00012-8.
[27] M.H.M. Oudshoorn, R. Rissmann, J.A. Bouwstra, W.E. Hennink, Synthesis of methacrylated hyaluronic acid with tailored degree of substitution, Polym. Guildf. 48 (2007) 1915–1920, http://dx.doi.org/10.1016/j.polymer.2007.01.068.
[28] S.A. Bencherif, A. Srinivasan, F. Horkay, J.O. Hollinger, K. Matyjaszewski, N.R. Washburn, Influence of the degree of methacrylation on hyaluronic acid hydrogels properties, Biomaterials 29 (2008) 1739–1749, http://dx.doi.org/10.1016/j.biomaterials.2007.11.047.
[29] Y.-H. Tsou, J. Khoneisser, P.-C. Huang, X. Xu, Hydrogel as a bioactive material to regulate stem cell fate, Bioact. Mater 1 (2016) 39–55, http://dx.doi.org/10.1016/j.bioactmat.2016.05.001.
[30] P. Jiang, Z. Mao, C. Gao, Combinational effect of matrix elasticity and alendronate density on differentiation of rat mesenchymal stem cells, Acta Biomater. 19 (2015) 76–84, http://dx.doi.org/10.1016/j.actbio.2015.03.018.
[31] G. Camci-Unal, D. Cuttica, N. Annabi, D. Demarchi, A. Khademhosseini, Synthesis and characterization of hybrid hyaluronic acid-gelatin hydrogels, Biomacromolecules 14 (2013) 1085–1092, http://dx.doi.org/10.1021/bm3019856.
[32] N.A. Peppas, J.Z. Hilt, A. Khademhosseini, R. Langer, Hydrogels in biology and medicine: from molecular principles to bionanotechnology, Adv. Mater 18 (2006) 1345–1360, http://dx.doi.org/10.1002/adma.200501612.
[33] W. Xiao, J. He, J.W. Nichol, L. Wang, C.B. Hutson, B. Wang, Y. Du, H. Fan, A. Khademhosseini, Synthesis and characterization of photocrosslinkable gelatin and silk fibroin interpenetrating polymer network hydrogels, Acta Biomater. 7 (2011) 2384–2393, http://dx.doi.org/10.1016/j.actbio.2011.01.016.
[34] P. Schumann, F. Tavassol, D. Lindhorst, C. Stuehmer, K.-H. Bormann, A. Kampmann, R. Mülhaupt, M.W. Laschke, M.D. Menger, N.-C. Gellrich, M. Rücker, Consequences of seeded cell type on vascularization of tissue engineering constructs in vivo, Microvasc. Res. 78 (2009) 180–190, http://dx.doi.org/10.1016/j.mvr.2009.06.003.
[35] A. Kampmann, D. Lindhorst, P. Schumann, R. Zimmerer, H. Kokemüller, M. Rücker, N.-C. Gellrich, F. Tavassol, Additive effect of mesenchymal stem cells and VEGF to vascularization of PLGA scaffolds, Microvasc. Res. 90 (2013) 71–79, http://dx.doi.org/10.1016/j.mvr.2013.07.006.
[36] Z. Fan, Y. Zhang, S. Fang, C. Xu, X. Li, Bienzymatically crosslinked gelatin/hyaluronic acid interpenetrating network hydrogels: preparation and characterization, RSC Adv. 5 (2015) 1929–1936, http://dx.doi.org/10.1039/C4RA12446D.
[37] T.I. Valdes, D. Kreutzer, F. Moussy, The chick chorioallantoic membrane as a novelin vivo model for the testing of biomaterials, J. Biomed. Mater. Res. 62 (2002) 273–282, http://dx.doi.org/10.1002/jbm.10152.